

# Investigation of $\text{In}_{0.53}\text{Ga}_{0.47}\text{As}/\text{AlAs}$ resonant tunneling diodes for high speed switching

D. H. Chow and J. N. S̄chulman  
*Hughes Research Laboratories, Malibu, California 90265*

E. Özbay and D. M. Bloom  
*Edward L. Ginzton Laboratory, Stanford University, Stanford, California 94305-4085*

(Received 14 February 1992; accepted for publication 27 July 1992)

We report an investigation of  $\text{In}_{0.53}\text{Ga}_{0.47}\text{As}/\text{AlAs}$  resonant tunneling diodes designed for high speed switching applications. Experimental peak current densities are observed to increase with decreasing AlAs barrier thicknesses, in good agreement with a two band tunneling calculation, which includes the effects of strain and band bending. Swing voltages over the range 0.5–1.0 V are demonstrated to be controllable via the thickness of a lightly doped depletion layer. Estimated RC time constants are compared with intrinsic tunneling times for the samples studied. A sample with 6 monolayer AlAs barriers yields devices with peak current densities of  $3.1 \times 10^5 \text{ A/cm}^2$  and peak-to-valley current ratios of 6:1. The minimum rise time in this sample is calculated to be limited by RC switching delays to 1.6 ps.

Resonant tunneling diodes (RTDs) are of interest for a number of high frequency applications due to their small characteristic dimensions. High speed switching, which utilizes the bistable RTD current-voltage ( $I$ - $V$ ) curve, is one of the most promising of these applications. RTD switching times on the order of 6 ps have been reported in GaAs/AlAs devices,<sup>1,2</sup> and triggering circuits based on RTD switching have been demonstrated up to frequencies of 110 GHz.<sup>3</sup>

Peak current density is the figure of merit for RTDs which is most crucial for switching speed.<sup>4</sup> Generally, the peak current density in a RTD can be increased by decreasing barrier thicknesses, up to a limit determined by device heating. As the need for high current densities necessitates low contact resistances and highly conductive cladding layers, InAs and InGaAs appear to be the best III-V electrode materials for this application.<sup>5-11</sup> InAs/AlSb RTDs have demonstrated peak current densities as high as  $3.7 \times 10^5 \text{ A/cm}^2$  and have produced oscillations at frequencies up to 712 GHz.<sup>5,6</sup> Extremely high peak current densities (up to  $4.5 \times 10^5 \text{ A/cm}^2$ ) have also been achieved in  $\text{In}_{0.53}\text{Ga}_{0.47}\text{As}/\text{AlAs}/\text{InAs}$  RTDs.<sup>7</sup> RTDs with InSb contact layers (another highly conductive material) have been demonstrated, but have not yet produced comparable results.<sup>12,13</sup>

A second important consideration for switching applications is the magnitude of the voltage swing between the peak and valley of the  $I$ - $V$  curve. This parameter, in combination with a choice of load resistance, determines the available drive voltage for switching (in a practical implementation, switching occurs from the peak of the  $I$ - $V$  curve to a point beyond the valley). The voltage swing can generally be controlled by varying the thickness of a lightly doped depletion layer on the positively biased side of an  $n$ -type RTD. This generalization holds provided that the depletion layer does not become thick enough to create significant series resistance due to electron storage (space charge transport). Unfortunately, large swing voltages in-

crease the RTD heat load, forcing a reduction in peak current densities.

In this letter, we report a study of  $\text{In}_{0.53}\text{Ga}_{0.47}\text{As}/\text{AlAs}$  RTDs for high speed switching applications. The samples investigated here were grown by molecular beam epitaxy in a Perkin Elmer 430P system on (100)-oriented InP substrates. The nominal substrate temperature for all of the samples was 520 °C. All of the structures were designed for reverse bias operation (negative bias on top of the structure). A description of the epitaxial layer sequence follows. Growth commenced with a 0.5  $\mu\text{m}$ ,  $n$ -type  $\text{In}_{0.53}\text{Ga}_{0.47}\text{As}$  contact layer, with  $n = 1.5 \times 10^{19} \text{ cm}^{-3}$ . This layer was followed by a lightly doped ( $n = 10^{17} \text{ cm}^{-3}$ )  $\text{In}_{0.53}\text{Ga}_{0.47}\text{As}$  layer, the thickness of which,  $d$ , was varied to control swing voltages. The double barrier region of the structure consisted of a 41 Å (14 monolayer)  $\text{In}_{0.53}\text{Ga}_{0.47}\text{As}$  quantum well sandwiched between two identical AlAs barriers and two 15 Å (5 monolayer) undoped  $\text{In}_{0.53}\text{Ga}_{0.47}\text{As}$  spacer layers. The AlAs barrier thickness,  $L_b$ , was varied to control current densities. The structure was completed by two 0.1  $\mu\text{m}$ ,  $n$ -type  $\text{In}_{0.53}\text{Ga}_{0.47}\text{As}$  contact layers, doped to  $10^{18} \text{ cm}^{-3}$  and  $1.5 \times 10^{19} \text{ cm}^{-3}$ , respectively. Structures similar to those described here have previously shown excellent device stability at elevated temperatures despite the large lattice mismatch of AlAs with respect to InP and  $\text{In}_{0.53}\text{Ga}_{0.47}\text{As}$ .<sup>10</sup> Table I contains the barrier and depletion layer thicknesses ( $L_b$  and  $d$ , respectively) used in the five samples grown for this study.

Fabrication of devices for this study was achieved via a simple one mask process. Grids of gold top contacts were defined by a standard photolithographic liftoff; the gold contacts were subsequently used to mask the sample during a wet chemical etch, creating mesa devices. The etch was stopped in the bottom  $\text{In}_{0.53}\text{Ga}_{0.47}\text{As}$  contact layer. "Back" contacts consisted of large area gold regions around the edge of each processed piece of material. Devices within each grid are identical in size and spaced by approximately 5  $\mu\text{m}$  to allow single device probing by a 1 mil (25  $\mu\text{m}$ ) gold wire set down randomly within the grid.

TABLE I. AlAs barrier thickness ( $L_b$ ), depletion layer thickness ( $d$ ), peak current density ( $J_p$ ), voltage swing ( $V_{\text{swing}}$ ), peak-to-valley current ratio ( $J_p/J_v$ ), estimated RC switching time ( $4R_nC$ ), and intrinsic tunneling time ( $t_{\text{int}}$ ), for four  $\text{In}_{0.53}\text{Ga}_{0.47}\text{As}/\text{AlAs}$  resonant tunneling structures.  $L_b$  and  $d$  are listed for a fifth structure, which burned out at voltages less than the peak voltage.

$L_b$ (mL)	$d$ (Å)	$J_p$ (kA/cm <sup>2</sup> )	$V_{\text{swing}}$ (V)	$J_p/J_v$	$4R_nC$ (ps)	$t_{\text{int}}$ (ps)
10	1000	11	1.0	28	41.0	8.2
8	1000	76	1.0	25	6.2	1.6
7	750	100	0.75	12	4.9	0.68
6	500	310	0.5	6	1.6	0.30
6	750	...	...	...	...	...

Device dimensions are varied from one grid to the next, with sizes ranging from 1.5  $\mu\text{m}$  squares to 20  $\mu\text{m}$  squares (2.25 to 400  $\mu\text{m}^2$ ).

Figure 1 is a room temperature  $I$ - $V$  curve taken from a 3.6  $\mu\text{m}$  square device on a sample with 8 monolayer AlAs barriers and a 1000 Å lightly doped  $\text{In}_{0.53}\text{Ga}_{0.47}\text{As}$  depletion layer. The curve displays a peak current density of  $7.6 \times 10^4$  A/cm<sup>2</sup> with a swing voltage of 1 V. The large swing voltage (wide valley region) is largely a result of the thick (1000 Å) depletion layer used in this sample. Figure 1 displays a peak-to-valley current ratio of 25:1; to the best of our knowledge, this value is the highest room temperature peak-to-valley ratio reported in any RTD with a peak current density above  $5 \times 10^4$  A/cm<sup>2</sup>. Figure 2 is a room temperature  $I$ - $V$  curve taken from 1.5  $\mu\text{m}$  square device on a sample with 6 monolayer AlAs barriers and a 500 Å lightly doped  $\text{In}_{0.53}\text{Ga}_{0.47}\text{As}$  depletion layer. The curve displays a peak current density of  $3.1 \times 10^5$  A/cm<sup>2</sup>. Due to the thinner depletion layer used in this sample, the swing voltage ( $=0.5$  V) is smaller than that observed in Fig. 1, but is still large enough to be practical for switching.

A theoretical model has been developed to simulate the  $I$ - $V$  behavior of these  $\text{In}_{0.53}\text{Ga}_{0.47}\text{As}/\text{AlAs}$  RTDs. The calculation is based on the two band model of Schulman and Waldner.<sup>14</sup> The tunneling through the AlAs barriers occurs in an energy region deep inside the AlAs band gap.

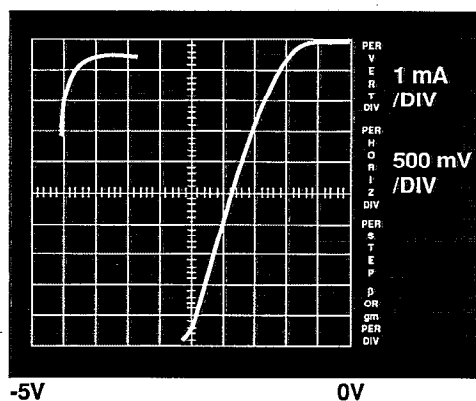


FIG. 1. Reverse bias current-voltage curve from: a  $3.6 \times 3.6 \mu\text{m}$  device on a sample with 8 monolayer AlAs barriers and a 1000 Å lightly doped  $\text{In}_{0.53}\text{Ga}_{0.47}\text{As}$  depletion layer. Figures of merit for the device are  $J_p = 7.6 \times 10^4$  A/cm<sup>2</sup>,  $J_p/J_v = 25$ , and  $V_{\text{swing}} = 1$  V.

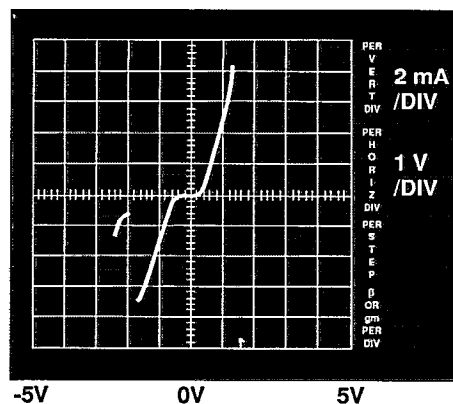


FIG. 2. Current-voltage curve from a  $1.5 \times 1.5 \mu\text{m}$  device on a sample with 6 monolayer AlAs barriers and a 500 Å lightly doped  $\text{In}_{0.53}\text{Ga}_{0.47}\text{As}$  depletion layer. Figures of merit for the device are  $J_p = 3.1 \times 10^5$  A/cm<sup>2</sup>,  $J_p/J_v = 6$ , and  $V_{\text{swing}} = 0.5$  V.

The energy versus imaginary wave vector band structure is therefore highly nonparabolic. It is important to include this nonparabolicity in the tunneling calculation; otherwise, the currents will be significantly underestimated. Strain effects on the thin AlAs barriers are straightforwardly incorporated into the tunneling calculation. Deformation potentials from the literature are used to shift the AlAs conduction band edge in the model, with effective masses scaled proportionally to the change in band gap. The valence band offset was assumed to be independent of strain. Finally, a Thomas-Fermi treatment of the band bending in the structures was employed to determine realistic band edge diagrams for the tunneling calculation.

Figure 3 contains a plot of the peak current densities measured from the first four samples listed in Table I as a function of AlAs barrier thickness in monolayers (1 monolayer  $\approx 2.7$  Å, including strain). Also plotted is the current density versus barrier thickness predicted by the previously described tunneling calculation (dashed line). Measured

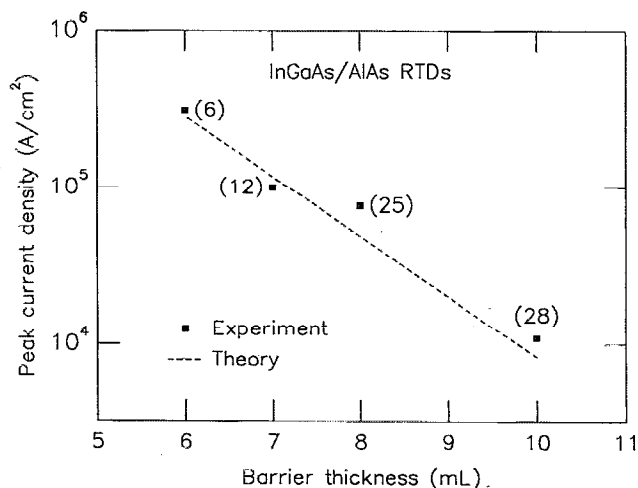


FIG. 3. Experimental (squares) and theoretical (dashed line) peak current density vs AlAs barrier thickness in  $\text{In}_{0.53}\text{Ga}_{0.47}\text{As}/\text{AlAs}$  resonant tunneling diodes. Measured peak-to-valley current ratios are given in parentheses next to the data points.

peak-to-valley current ratios are included in parentheses next to the data points in the figure. The current density is observed to rise exponentially (within experimental uncertainties) with decreasing barrier thickness, in good agreement with the tunneling calculation. Devices tested on the fifth sample listed in Table I burned out before the negative differential resistance region could be reached. This sample differs from the fourth sample listed in Table I (whose current-voltage characteristic is shown in Fig. 2) only in the thickness of its depletion layer,  $d$ , which is 750 instead of 500 Å. The burnout of the devices in the fifth sample is attributable to the increase in voltage drop (hence greater power generation) across the depletion layer. Swing voltages for the first four samples are listed in Table I, displaying a monotonic decrease with decreasing values of  $d$ .

In addition to the current density and swing voltage data listed in Table I, we have estimated RC and intrinsic switching times for the first four samples in the table. The RC times are estimated via the analysis of Ref. 4, which found that the minimum obtainable rise time in a RTD is approximately  $4R_nC$ , where  $R_n$  is the average negative resistance, i.e., swing voltage divided by available current, and  $C$  is the device capacitance.<sup>4</sup> The intrinsic times are estimated by computing the width of the transmission coefficient peak at resonance and applying the uncertainty principle. The transmission coefficient was obtained via the tunneling calculation used to generate the dashed line in Fig. 3. A third characteristic time, the depletion layer transit time, is estimated to be subpicosecond for all of the samples studied here. For all four samples, the RC switching time is greater than the intrinsic time, although the difference is less than one order of magnitude. The fourth sample listed in Table I has an estimated RC switching time of  $4R_nC = 1.6$  ps, and an intrinsic response time of 300 fs.

It should be noted that Ref. 15 predicts subpicosecond switching times for InGaAs/AlAs/InAs RTDs based on the data reported in Ref. 7. However, swing voltages in those cases were uncomfortably small for switching applications. As discussed previously, the trade-off between swing voltage and device heating necessitates some compromise in switching speed for practical swing voltages. The present work indicates that this trade off can be made without foregoing picosecond switching times in In<sub>0.53</sub>Ga<sub>0.47</sub>As/AlAs RTDs.

In summary, we have investigated the suitability of In<sub>0.53</sub>Ga<sub>0.47</sub>As/AlAs resonant tunneling diodes for ultrafast switching. Peak current densities were observed to depend exponentially on AlAs barrier thickness, in good agreement with the predictions of a two band tunneling model. Practical swing voltages, ranging from 0.5 to 1.0 V, were demonstrated to be controllable via the thickness of a

lightly doped depletion layer. Emphasis in layer design was placed on the attainment of high peak current densities; nevertheless the devices yielded extremely high peak-to-valley current ratios. A sample with 8 monolayer AlAs barriers yielded a peak-to-valley current ratio of 25 with a peak current density of  $7.6 \times 10^4$  A/cm<sup>2</sup>, while a sample with 6 monolayer AlAs barriers yielded a peak current density of  $3.1 \times 10^5$  A/cm<sup>2</sup> with a peak-to-valley ratio of 6. The minimum switching time of the latter device is estimated to be 1.6 ps, with RC time as the limiting factor. Our results indicate that In<sub>0.53</sub>Ga<sub>0.47</sub>As/AlAs RTDs are an excellent choice for switching applications in the few picosecond range.

The authors gratefully acknowledge helpful discussions with H. Dunlap, T. C. Hasenberg, E. T. Croke, R. H. Miles, A. T. Hunter, M. H. Young, D. A. Collins (Caltech), and T. C. McGill (Caltech). R. E. Doty performed scanning electron microscope work for this study. Vital technical assistance was provided by L. D. Warren and C. Haeussler. The Stanford portion of this work was funded by DARPA managed by NOSC under subcontract from the Mayo Foundation on Contract No. N66001-89-C-0104 and by the SDIO/IST managed by ONR under Contract No. N00014-89-K-0067.

- <sup>1</sup>J. F. Whitaker, G. A. Mourou, T. C. L. G. Sollner, and W. D. Goodhue, *Appl. Phys. Lett.* **53**, 385 (1988).
- <sup>2</sup>E. Özbay, S. K. Diamond, and D. M. Bloom, *Electron. Lett.* **26**, 1046 (1990).
- <sup>3</sup>E. Özbay and D. M. Bloom, *IEEE Electron Device Lett.* **12**, 480 (1991).
- <sup>4</sup>S. K. Diamond, E. Özbay, M. J. W. Rodwell, D. M. Bloom, Y. C. Pao, and J. S. Harris, *Appl. Phys. Lett.* **54**, 153 (1989).
- <sup>5</sup>J. R. Söderström, E. R. Brown, C. D. Parker, L. J. Mahoney, J. Y. Yao, T. G. Andersson, and T. C. McGill, *Appl. Phys. Lett.* **58**, 275 (1991).
- <sup>6</sup>E. R. Brown, J. R. Söderström, C. D. Parker, L. J. Mahoney, K. M. Molvar, and T. C. McGill, *Appl. Phys. Lett.* **58**, 2291 (1991).
- <sup>7</sup>T. P. E. Broekaert and C. G. Fonstad, *Proceedings of the International Electron Devices Meeting*, 1989, p. 559.
- <sup>8</sup>T. P. E. Broekaert, W. Lee, and C. G. Fonstad, *Appl. Phys. Lett.* **53**, 1545 (1988).
- <sup>9</sup>Y. Sugiyama, T. Inata, S. Muto, Y. Nakata, and S. Hiyamizu, *Appl. Phys. Lett.* **52**, 314 (1988).
- <sup>10</sup>A. Miura, T. Yakhara, S. Uchida, S. Oka, S. Kobayashi, H. Kamada, and M. Dobashi, *IEEE Trans. Microwave Theory Tech.* **38**, 1980 (1990).
- <sup>11</sup>R. M. Kapre, A. Madhukar, and S. Guha, *Appl. Phys. Lett.* **58**, 2255 (1991).
- <sup>12</sup>J. R. Söderström, J. Y. Yao, T. G. Andersson, *Appl. Phys. Lett.* **58**, 708 (1991).
- <sup>13</sup>J. Han, S. M. Durbin, R. L. Gunshor, M. Kobayashi, D. R. Menke, N. Pelekanos, M. Hagerott, A. V. Nurmikko, Y. Nakamura, and N. Otsuba, *J. Cryst. Growth* **111**, 767 (1991).
- <sup>14</sup>J. N. Schulman and M. Waldner, *J. Appl. Phys.* **63**, 2859 (1988).
- <sup>15</sup>E. R. Brown, C. D. Parker, A. R. Calawa, M. J. Manfra, T. C. L. G. Sollner, C. L. Chen, S. W. Pang, and K. M. Molvar, *Proc. SPIE* **1288**, 122 (1990).